THE IMPACT OF ALLOY COMPOSITION ON SHEAR STRENGTH FOR LOW TEMPERATURE LEAD FREE ALLOYS

Traian C. Cucu, Ph.D., Carl Bilgrien, Ph.D., Anna Lifton, Irina Lazovskaya
Alpha Assembly Solutions, a MacDermid Performance Solutions Business
South Plainfield, NJ, USA
Traian.Cucu@alphaassembly.com

ABSTRACT

The low temperature assembly processes are continuing to rise in popularity throughout the assembly industry and the Sn-Bi based alloys act as an enabler for this transition. The use of a lower assembly temperature (lower peak, lower thermal energy used during the assembly process) brings a sum of benefits: Lower expansion/shrinkage due to CTE mismatch, reduced dynamic warpage, lower thermal stress during the assembly process and the use of environmental friendly processes. There is a plethora of different materials that are used to manufacture the boards and the parts that get assembled on the boards and they all have very different coefficients of thermal expansion (CTE). As these assemblies, undergo temperature/power changes during use (equipment switching on/off, day and night temperature changes, etc.) CTE mismatch causes added stress and strain on the solder joint. Increase in strain could result in solder joint degradation that ultimately will lead to joint failure (crack initiation and propagation through the solder joint fillet. The next generation of low temperature (LT) solder pastes recently introduced to the market makes use of new low temperature alloys (LTA) and new chemistry platforms These innovations have brought the LTA joint mechanical performance nearly to the performance of a Sn-Ag-Cu (SAC) joint. The new alloy considered for this paper (X46) is a Sn-Bi system with micro-additives that further improve the base alloy properties, bringing its performance within SAC305 performance.

In this paper the mechanical performance of the joint is characterized using the shear test for passive components. This measurement is looking at the joints formed with the alloy by itself. In order to simulate the induced stress caused by the CTE mismatch occurring during the normal operation in the field, the test boards were put through two thermal stress regimes: thermal cycling (TC) and thermal stress (TS). The shear test was performed after predefined number of cycles, for both TC and TS in order to generate the degradation curve for the given joint. Different reflow profiles have been employed for the LTA, to further define the process window for a given alloy (shear resistance degradation).

Key words: Lead-free, low temperature soldering, shear force, thermal-stress, thermal-cycling, CTE mismatch, reflow process window.

INTRODUCTION

Low temperature processing has been an assembly industry objective ever since the transition from leaded to lead free alloys [1]. As the lead-free assembly process reached its maturity, the LTA and the low temperature assembly process became more appealing, due to the benefits they bring to the final assembly. The LTA, as a replacement for the SAC alloys, have driven multiple research programs in the industry, all aimed to develop LTA and low temperature solder pastes that can fit existing assembly processes with minimal changes in the existing processes [2] – [5]. The new LT alloys and solder pastes allow, among other things, the reduction of the thermal energy needed during the reflow process, and consequently, the use of a lower peak and a "colder" reflow profile. This has a positive impact on the components and boards behavior, as it reduces the expansion/shrinkage due to CTE mismatch, reduces the dynamic warpage, exerts lower thermal stress during the assembly process and improves the production yields [6] - [7]. LT materials with mechanical and thermal performance close to or better than SAC alloys allow the use of multi-step assembly process. [5] The "step-down" in the process temperatures ensures that the previously formed jointwill not reach the melting point again. Fig.1 shows an alloy classification based on the peak temperature of the reflow process [1].

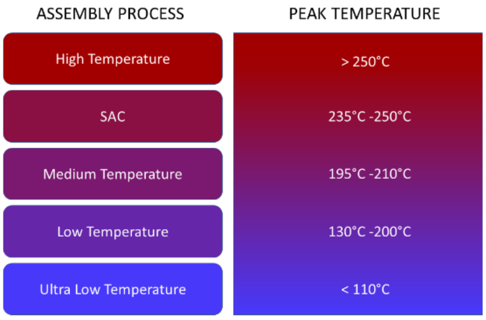

ASSEMBLY PROCESS	PEAK TEMPERATURE
High Temperature	> 250°C
SAC	235°C -250°C
Medium Temperature	195°C -210°C
Low Temperature	130°C -200°C
Ultra Low Temperature	< 110°C

Figure 1. Classification of the Assembly Process Based on the Peak Reflow Temperature

In Table 1 we have the melting ranges for the alloys used in the experiments carried out to generate the data presented in this paper.

Table 1. Melting Ranges for the Alloys Considered for the Experimental Work

Alloy	Alloy Composition [%]	Solidus Temp. [°C]	Liquidus Temp. [°C]	Delta [°C]
SAC305	Sn96.5 Ag3.0 Cu0.5	217	220	3
SnBi0.4Ag	Sn42Bi57.6Ag0.4	138	138	0
SBX02	SnBi+additives	139	139	0
X46	SnBi+additives	138	151	13

Considering the wider plastic range for X46 alloy we used three reflow profiles when components were assembled with a solder paste using the X46 alloy.

In order to minimize variations in the data, the same equipment and the same test vehicle design were used for all solder pastes (identical pad size and design, OSP surface finish), and a 100% fillet height was targeted for all deposits, Fig.2.

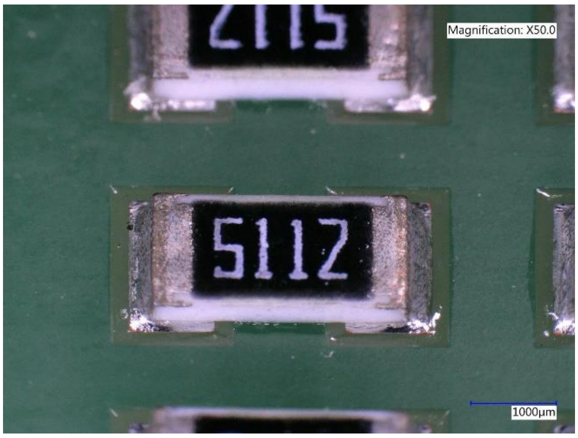

Figure 2. Fillet Height for a 1206 Chip resistor

EXPERIMENT DESCRIPTION

Printing Process

The boards were produced on an automated line. For the printing step a Dek Horizon printer was used with a stainless steel, laser cut stencil, with a 5 mil thickness. Table 2 presents the printing parameters used in the process. The visual inspection after the printing process was carried out on a Keyence microscope and paste volumes were measured using a Koh Young equipment. Fig.3 shows paste deposits for a 1206 chip resistor, in Fig.4 shows a rendered image of a paste deposit, as generated by the measuring equipment.

Table 2. Printing parameters

Print Speed	30 mm/s	
Print Pressure	66 N (1.5 lbs/inch, 250 mm blade)	
Stencil Release	15 mm/s	
Squeegee Angle	45 degrees	
Wipe	Dry Vacuum Wipe after every 2 prints	

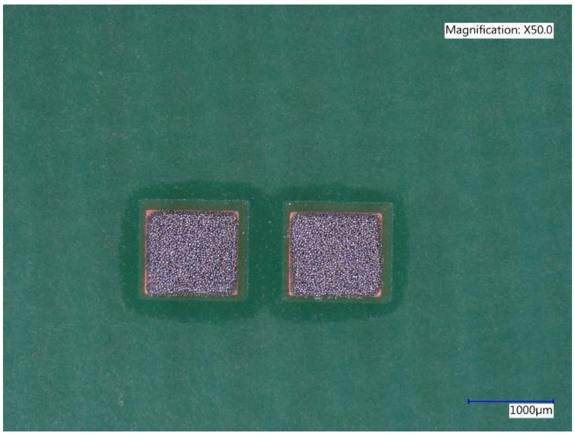

Figure 3. Solder Paste Deposits for a 0603 Chip Resistor

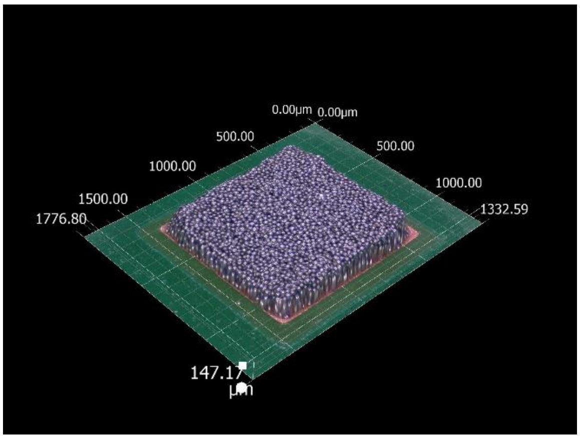

Figure 4. Rendered Image of a Paste Deposit for 0603 Pad

Reflow Process

Different reflow profiles were used based on the specific alloys. Fig.5 shows the reflow profile used for the solder paste with SAC305, and Fig.6 shows the reflow profile used for the solder paste with Sn42Bi57.6Ag0.4 alloy (eutectic LTA).

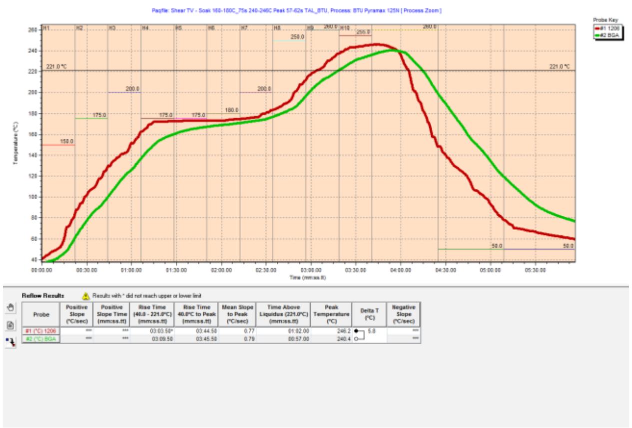

Reflow Results ⚠ Results with * did not reach upper or lower limit

Probe	Positive Slope (°C/sec)	Positive Slope Time (mm:ss.tt)	Rise Time (40.0 - 221.0°C) (mm:ss.tt)	Rise Time 40.0°C to Peak (mm:ss.tt)	Mean Slope to Peak (°C/sec)	Time Above Liquidus (221.0°C) (mm:ss.tt)	Peak Temperature (°C)	Delta T (°C)	Negative Slope (°C/sec)
#1 (°C) 1206	***	***	03:03.50*	03:44.50	0.77	01:02.00	246.2	5.8	***
#2 (°C) BGA	***	***	03:09.50	03:45.50	0.79	00:57.00	240.4		***

Figure 5. SAC305 Reflow Profile

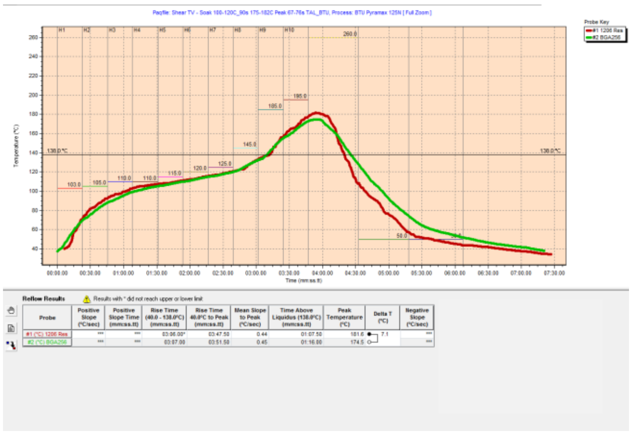

Reflow Results Results with * did not reach upper or lower limit

Probe	Positive Slope (°C/sec)	Positive Slope Time (mm:ss.ttt)	Rise Time (40.0 - 138.0°C) (mm:ss.ttt)	Rise Time 40.0°C to Peak (mm:ss.ttt)	Mean Slope to Peak (°C/sec)	Time Above Liquidus (138.0°C) (mm:ss.ttt)	Peak Temperature (°C)	Delta T (°C)	Negative Slope (°C/sec)
#1 (°C) 1206 Res	***	***	03:06.00*	03:47.50	0.44	01:07.50	181.6	7.1	***
#2 (°C) BGA256	***	***	03:07.00	03:51.50	0.45	01:16.00	174.5		***

Figure 6. Sn42Bi57.6Ag0.4 Reflow Profile

For the solder paste using the X46 alloy (off-eutectic LTA) we used three different profiles, Table 3 and Fig.7. This was considered in order to expose the influence of the peak temperature, if any.

Table 3. Reflow Settings for Alloys in Test

	Time to Peak [sec.]	TAL [sec]	Peak Temp. [°C]
Profile 1 - X46	233	80-85	181°C
Profile 2 - X46	238	80-85	195°C
Profile 3 - X46	235	80-85	211°C
Sn42Bi57.6Ag0.4	227	67-76	182
SAC305	225	57-60	246

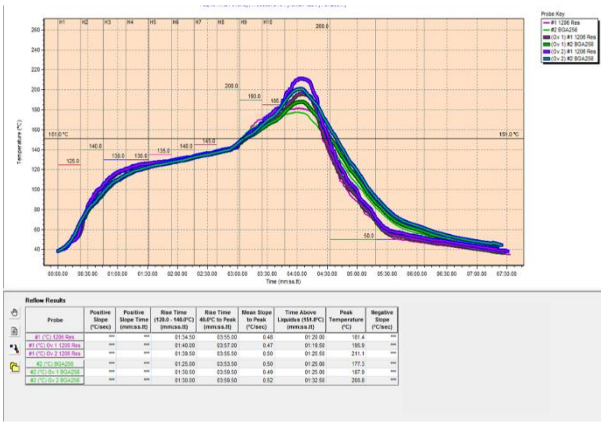

Reflow Results

Probe	Positive Slope (°C/sec)	Positive Slope Time (mm:ss.tt)	Rise Time (120.0 - 140.0°C) (mm:ss.tt)	Rise Time 40.0°C to Peak (mm:ss.tt)	Mean Slope to Peak (°C/sec)	Time Above Liquidus (151.0°C) (mm:ss.tt)	Peak Temperature (°C)	Negative Slope (°C/sec)
#1 (°C) 1206 Res	***	***	01:34.50	03:55.00	0.48	01:20.00	181.4	***
#1 (°C) Ov 1 1206 Res	***	***	01:40.00	03:57.00	0.47	01:19.50	195.9	***
#1 (°C) Ov 2 1206 Res	***	***	01:39.50	03:55.50	0.50	01:25.50	211.1	***
#2 (°C) BGA256	***	***	01:25.00	03:53.50	0.50	01:25.00	177.3	***
#2 (°C) Ov 1 BGA256	***	***	01:30.50	03:59.50	0.49	01:25.00	187.9	***
#2 (°C) Ov 2 BGA256	***	***	01:30.00	03:59.50	0.52	01:32.50	200.8	***

Figure 7. Reflow Profiles for X46 Alloy

Testing Procedure

The Thermal Cycle (TC) and Thermal Shock (TS) regimes are showed in Table 4.

TC	-40°C/+125°C	20 min dwell, 10 min ramp
TS	-40°C/+125°C	3 min dwell, 10s transfer

Table 4. TC and TS regimes

For the TC, boards were taken out of the chamber at 500, 1000, 1500 and 2000 cycles. For TS, boards were taken out of the chamber at 100, 500 and 1000 cycles.

Shear force measurements were taken using a XYZtec Sigma Condor Die Shear system. Due to the solder mask thickness and relatively low bond line thickness (BLT) of the chip components the shear height of the system was set to 10 microns. The system was programmed to shear through 1000 um (1 mm) and hold for 2 seconds at the maximum deflection. Samples were presented to the system individually and the stage was adjusted to ensure that the shear blade was parallel with the face of the component. Peak shear force was the primary parameter of interest that was measured for all components tested. Destructive shear force tests were performed at 0, 500, 1000, 1500, and 2000 cycles, for the boards that were exposed to TC and at 0, 100, 500 and 1000 cycles for the boards exposed to TS.

RESULTS AND DISCUSSION

The SAC305 and Sn42Bi57.6Ag0.4 materials have been used as benchmarks in all three situations when three different reflow profiles have been used for the X46 alloy. An average value has been calculated from the discrete values measured for each instance during testing.

The graphical representations of the average shear force values are shown in Fig.7 – Fig.12.

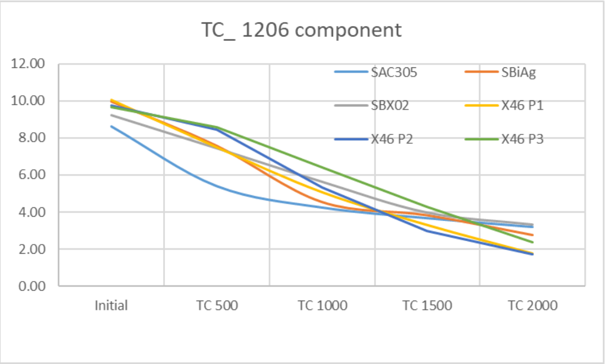

Figure 7. Shear Force for 1206 Component - TC

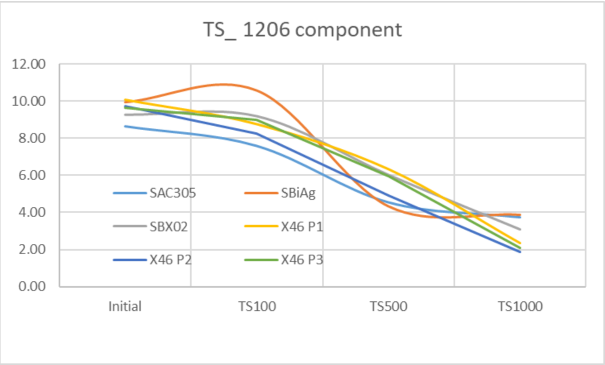

Figure 8. Shear Force for 1206 Component - TS

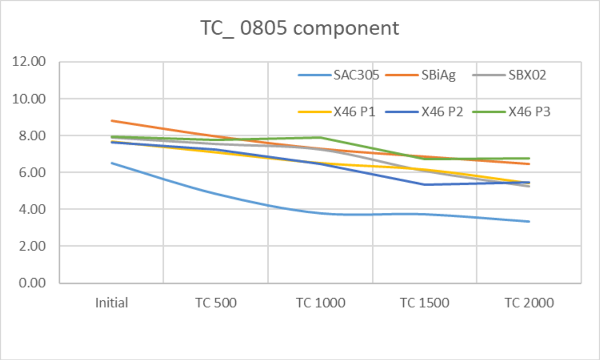

Figure 9. Shear Force for 0805 Component - TC

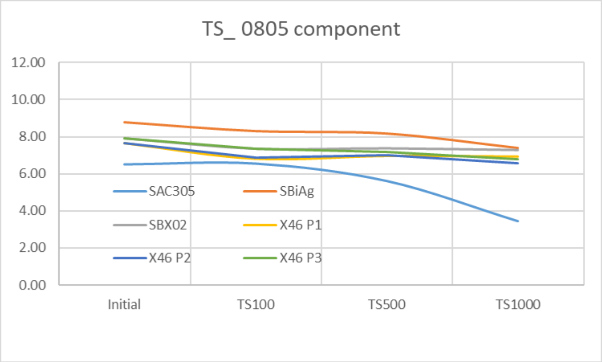

Figure 10. Shear Force for 0805 Component - TS

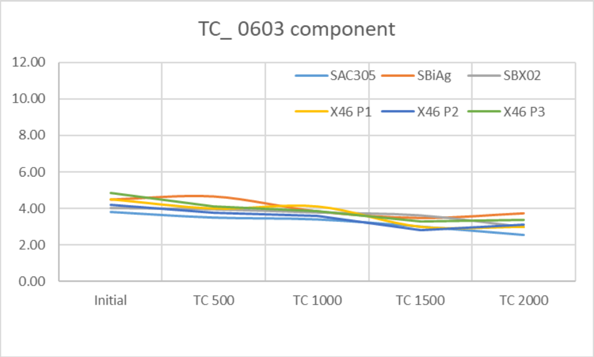

Figure 11. Shear Force for 0603 Components - TC

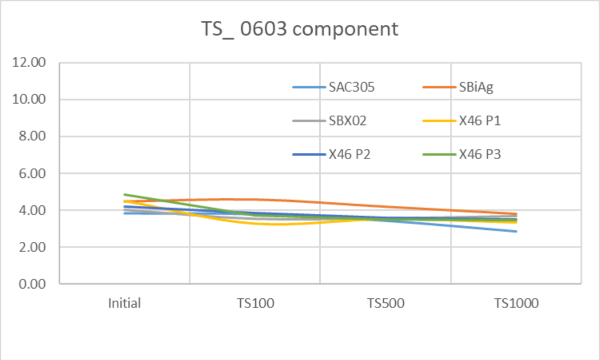

Figure 12. Shear Force for 0603 components - TS

Joint degradation as the boards are going through the two thermal cycles happened for all the alloys in test, yet there was a different trend observed for the SAC305 versus the LTA. This can be attributed to the way the intermetallic layer is formed during the initial reflow process and the way it grows during the thermal aging. SAC305 forms a complex intermetallic structure along the interface, and this structure grows significantly during the thermal excursions when compared with the LTA. There were differences in performance observed when moving from one component size to another, which is attributed to the influence the volume of solder in each joint will have. We have seen two types of failure modes: Fractures through the IMC layer and through the bulk. Based on the analyses of the rupture area and the intermediate cross sections, we concluded that the majority of the failures could be attributed to initial cracks formed at the IMC layer level These will later have a bi-modal propagation through the IMC layer or through the bulk of the joint. These fissures (an extreme example is demonstrated in Fig. 13) will have a decisive contribution to the performance of the joint during TC and TS.

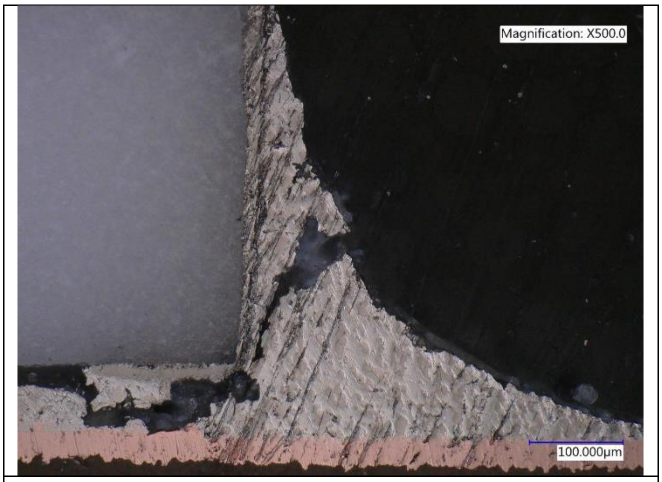

Figure 13. Cross-section 1206 chip after 500 cycles TS

CONCLUSIONS

The mechanical degradation of the joints formed with a set of LTA has been studied using SAC305 as a benchmark. The best overall performer was an alloy with micro-additives, with the alloy composition optimized for higher performance. The results suggest that selective addition of micro-additives can yield higher thermal-mechanical performance of the joint performance.

For the LTA in the test, as demonstrated for the LTA with micro-additives (X46) the mechanical degradation of a joint subjected to a thermal cycling type of stress, can be improved by both alloy design and by fine-tuning the assembly process (the reflow profile used to form the joint). The X46 alloy exhibited a high flexibility, showing good results (better than or equal to the benchmark) for all three thermal envelopes used in the assembly process. This suggests that it has a wide process window during the assembly process that allows its use in both joints formed with the alloy by itself and mixed joints.

The shear strength degradation for the LTA (high Bi alloy) is lower for the alloy optimized through the addition of micro-additives, and it shows that the optimized composition has an influence on the alloy performance. The reasons and mechanisms of this are out of the scope of this paper and it is a theme that is proposed for further studies.

ACKNOWLEDGEMENTS

Big thanks to our colleagues from America R&D Center for their contributions to this body of work. We also want to thank other colleagues from CTS, Marketing and Sales that have participated in discussions related to this body of work. All contributions were important and eventually helped in defining the experiments that generated the data for this manuscript.

REFERENCES

[1] M. Ribas, T. Hunsinger, T. Cucu, H.V. Ramakrishna, G. Lim, M. Murphy, The Printed Circuit Assembler/s Guide to Low-Temperature Soldering, 2018, Retrieved from http://i007ebooks.com/my-i-connect007/books/lts/.

[2] H. Fu, R. Aspandiar, J. Chen, S. Cheng, Q. Chen, R. Coyle, S. Feng, M. Krmpotich, R. Lasky, S. Mokler, J. Radhakrishnan, M. Ribas, B. Sandy-Smith, K. K. Tang, G. Wu, A. Zhang, and W. Zhen, "iNEMI Project on Process Development of BiSn-Based Low Temperature Solder Pastes", Proceedings of the 2017 SMTA International Conference, Rosemont, IL, September 2017, 207-220.

[3] H. Fu, R. Aspandiar, J. Chen, S. Cheng, Q. Chen, R. Coyle, S. Feng, B. Hardin, M. Krmpotich, S. Mokler, J. Radhakrishnan, M. Ribas, B. Sandy-Smith, K. K. Tang, G. Wu, A. Zhang, and W. Zhen, "iNEMI Project on Process Development of BiSn-Based Low Temperature Solder Pastes – Part II: Characterization of Mixed Alloy BGA Solder Joints", Proceedings of the 2018 Pan Pacific Microelectronics Symposium, Hawaii, February 2018.

[4] H. Fu, J. Radhakrishnan, M. Ribas, R. Aspandiar, K. Byrd, J. Chen, S. Cheng, Q. Chen, R. Coyle, S. Feng, B. Hardin, M. Krmpotich, S. Mokler, B. Sandy-Smith, K. K. Tang, G. Wu, A. Zhang, and W. Zhen, "iNEMI Project on Process Development of BiSn-Based Low Temperature Solder Pastes – Part III: Mechanical Shock Tests on POP BGA Assemblies", Proceedings of the 2018 International Conference on Electronics Packaging, Kuwana, Japan, April 2018.

[5] T.C. Cucu, I. Plotog, P. Svasta, M. Branzei, Low Silver, Lead Free Solder Paste, New Alloy Developments, SIITME 2010, 16th International Symposium for Design and Technology in Electronic Packaging, September 23-26, 2010.

[6] Aspandiar, R., Byrd, K., Tang, K. K., Campbell, L., and Mokler, S., "Investigation of Low-temperature Solders to Reduce Reflow temperature, Improve SMT Yields and Realize Energy Savings." Proceedings of the IPC APEX EXPO. San Diego, California. February 2015.

[7] Mokler, S., Aspandiar, R., Byrd, K., Chen, O., Walwadkar, S., Tang, K. K., Renavikar, M., and Sane, S., "The Application of Bi-Based Solders for Low-temperature Reflow to Reduce Cost While Improving SMT Yields in Client Computing Systems." Proceedings of the SMTA International Conference and Exhibition. Rosemont, Illinois. September 2016.